Analysis of the demagnetization process of Nd–Fe–B sintered magnets at elevated temperatures by magnetic domain observation using a Kerr microscope

M. Takezawa, H. Ogimoto, Y. Kimura, and Y. Morimoto

Citation: Journal of Applied Physics **115**, 17A733 (2014); doi: 10.1063/1.4866894
View online: http://dx.doi.org/10.1063/1.4866894
View Table of Contents: http://scitation.aip.org/content/aip/journal/jap/115/17?ver=pdfcov
Published by the AIP Publishing

Analysis of the demagnetization process of Nd–Fe–B sintered magnets at elevated temperatures by magnetic domain observation using a Kerr microscope

M. Takezawa,[a] H. Ogimoto, Y. Kimura, and Y. Morimoto
Department of Applied Science for Integrated System Engineering, Faculty of Engineering, Kyushu Institute of Technology, 1-1 Sensui-cho, Tobata-ku, Kitakyushu, Fukuoka 804-8550, Japan

(Presented 5 November 2013; received 23 September 2013; accepted 25 November 2013; published online 25 February 2014)

Magnetization reversal and its propagation in sintered Nd–Fe–B magnets were clearly observed at elevated temperatures up to 150 °C using a Kerr microscope, image processing, and photo editing. Simultaneous magnetization reversal in several grains along the easy axis direction occurred at elevated temperature, and the extent of simultaneous magnetization reversal increased with temperature. This indicates that reduction in the coercivity of Nd–Fe–B sintered magnets at elevated temperatures is attributable to decrease in anisotropy and insufficient pinning of domain walls at grain boundaries. © *2014 AIP Publishing LLC*. [http://dx.doi.org/10.1063/1.4866894]

I. INTRODUCTION

Electrical vehicles require heat-resistant Nd–Fe–B high-coercivity magnets. Because thermal stability up to temperature of 200 °C is required for electrical vehicles, a very high coercivity of 30 kOe is necessary at room temperature. Therefore, to enhance coercivity, commercially available Nd–Fe–B magnets containing a large amount of the rare metal Dysprosium (Dy) are used.[1,2] However, low natural abundance of Dy is a crucial resource problem. A Kerr microscope is useful for *in situ* domain observations of high magnetic fields at high temperatures.[3,4] Through domain observation using an *in-situ* Kerr microscope, we have previously reported that the extent of the simultaneous magnetization-reversal area is related to the coercivity of Nd–Fe–B sintered magnets.[5] In this study, we examine the magnetization process at elevated temperatures by an image-processing technique using a Kerr microscope in order to clarify the reason for decrease in the coercivity of sintered Nd–Fe–B magnets at elevated temperatures through domain observation.

II. EXPERIMENTAL DATA

The magnetic domain of commercially available Nd–Fe–B sintered magnet for a voice coil motor was observed using a Kerr microscope. The intrinsic coercivity of the sample was approximately 14 kOe. The magnet was cut into samples 3.5 mm thick, 9.0 mm long, and 5.0 mm wide, and the sample surfaces were polished to clearly reveal the domain configuration during experiments. The magnets were cut at an angle of 10° to c-axis to obtain information about the domain configuration underneath the surface, as described elsewhere.[6] A Tantalum (Ta) thin film was deposited by RF sputtering on surface of the Nd–Fe–B sintered magnets to prevent oxidation. Then, a SiO thin film was also deposited on the Ta thin film by vacuum evaporation and functioned as an antireflection coating.

The Kerr microscope was built in a temperature-controlled stage with an electromagnet that produced a high magnetic field up to 14.2 kOe. The demagnetization process of a previously magnetized magnet was accomplished with a pulse field of +50 kOe. The magnetization/demagnetization process was observed by applying a DC field from +14.2 to −14.2 kOe along the easy axis direction of the magnet, and the samples were evaluated from 25 °C to 150 °C. For detailed observation of magnetization reversal at elevated temperatures, we derived the domain change by subtracting the domain image in an applied field from that in another applied field using a photo-editing application.[5]

III. RESULTS AND DISCUSSION

Figure 1 shows domain images of an Nd–Fe–B sintered magnet sample when a DC field from +14.2 to −14.2 kOe was applied along the longitudinal direction at room

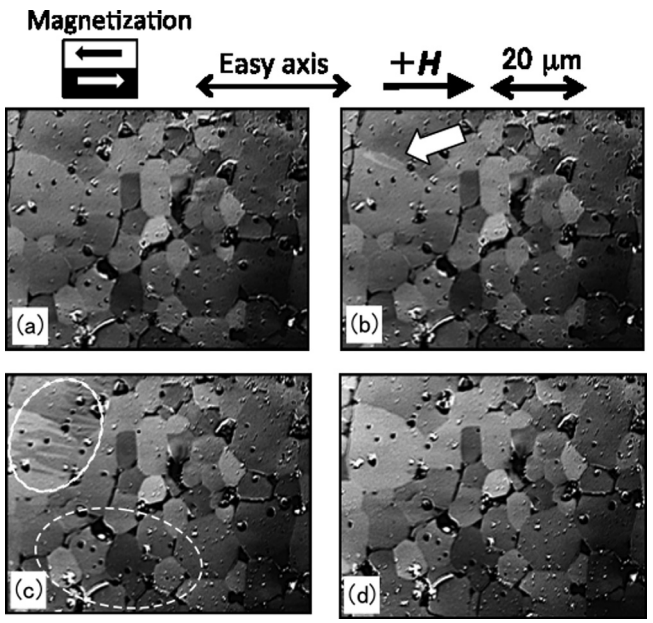

FIG. 1. Magnetic domain images at 25 °C with an applied DC field of: (a) +2.0 kOe, (b) +1.7 kOe, (c) 0, and (d) −4.0 kOe.

[a]Electronic mail: take@ele.kyutech.ac.jp.

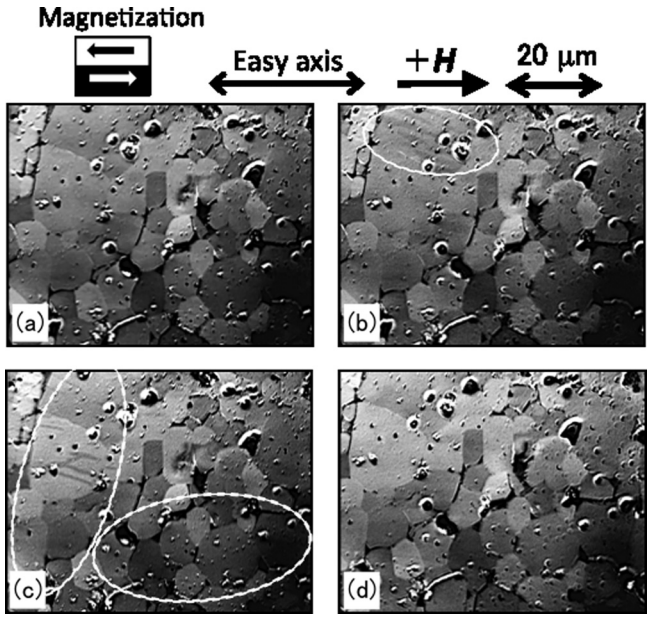

FIG. 2. Magnetic domain images at 60 °C with an applied DC field of: (a) +1.0 kOe, (b) +0.5 kOe, (c) −0.1 kOe, and (d) −3.0 kOe.

temperature (25 °C). The bright and dark domains are magnetized in leftward and rightward directions, respectively. The grain size is about 10 μm. When the DC field was decreased from +14.2 kOe to +2.0 kOe in the rightward direction, all grains exhibited dark domains having rightward magnetization components (Fig. 1(a)). The data indicate that a saturated state was obtained at that field value. When the DC field was decreased to +1.7 kOe, the reversed domains nucleated, and the domain structure changed from a single domain state to a multi-domain state in one grain, as indicated by the arrow in Fig. 1(b). The reversed domains grew when the DC field was changed to 0, marked by the solid line ellipse in Fig. 1(c). Simultaneous magnetization reversal in several grains beyond the grain boundaries along the easy axis direction was also observed when the DC field was reduced to zero, marked by the dotted-line ellipses in Fig. 1(c). When the DC field reached −4.0 kOe, all grains, exhibiting bright domains, were inversely saturated (Fig. 1(d)).

Figure 2 shows domain images of the Nd–Fe–B sintered magnet at an elevated temperature of 60 °C. Figure 2(a) shows that saturation occurred at +1.0 kOe. The domain structure changed from a single domain state to a multi-domain state in some grains at +0.5 kOe, marked by the ellipse in Fig. 2(b). When the DC field changed to −0.1 kOe, the reversed domains grew and simultaneous magnetization reversal in several grains was observed, as marked by the

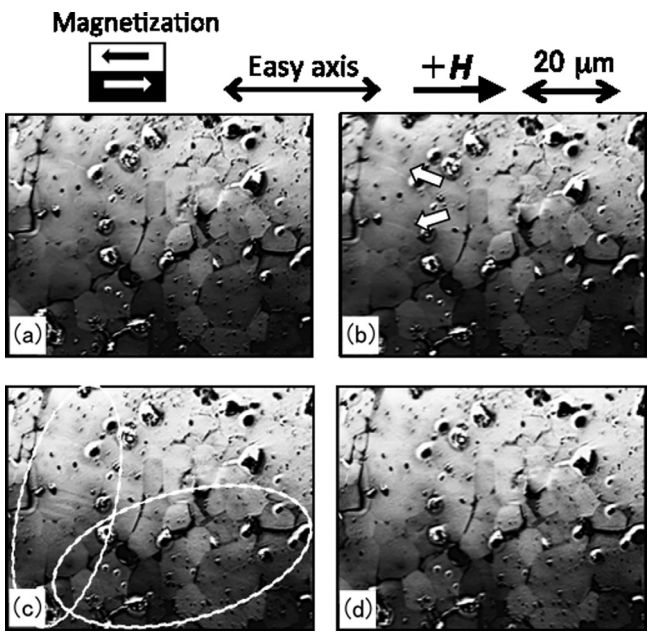

FIG. 3. Magnetic domain images at 150 °C with an applied DC field: (a) +2.0 kOe, (b) +1.5 kOe, (c) +1.3 kOe, and (d) 0 kOe.

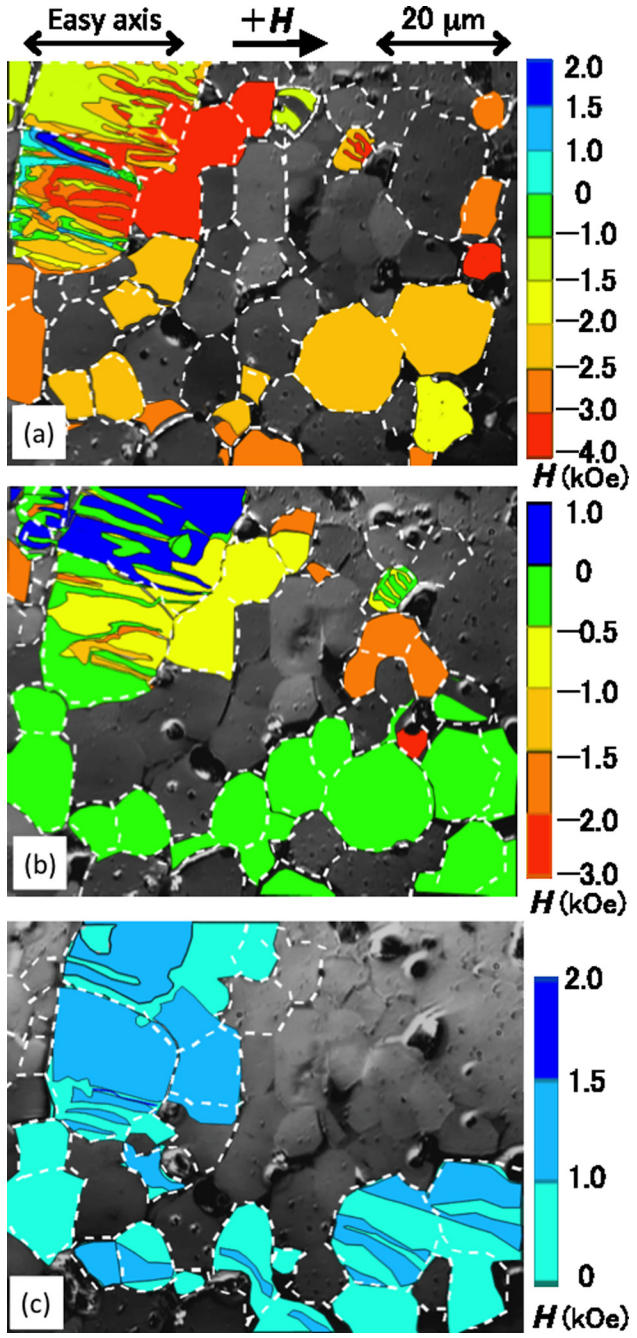

FIG. 4. Processed images indicating the area of magnetization reversal at: (a) 25 °C, (b) 60 °C, and (c) 150 °C.

ellipse in Fig. 2(c). All grains were inversely saturated at −3.0 kOe (Fig. 2(d)), a lower negative field than the inverse saturation field at room temperature.

Figure 3 shows domain images of the Nd–Fe–B sintered magnet at an elevated temperature of 150 °C. Figure 3(a) shows that saturation occurred at +2.0 kOe. Nucleation of the reversed domain appeared at a DC field of +1.5 kOe at 150 °C, as indicated by the arrow in Fig. 3(b). When the DC field changed to +1.3 kOe, the reversed domains grew and simultaneous magnetization reversal in several grains was observed, marked by the ellipse in Fig. 3(c). All grains were inversely saturated at a field value of zero (Fig. 3(d)), a lower negative field than the inverse saturation field strengths at 60 °C and 25 °C.

Figure 4 shows the image-processed domain images indicating the magnetization-reversal area for each magnetic field strength at temperatures of 25 °C, 60 °C, and 150 °C. The simultaneous magnetization reversal in a few grains occurred with an applied DC field from −2.0 to −4.0 kOe at room temperature, as shown in Fig. 4(a). On the other hand, at 60 °C, the simultaneous magnetization reversal in several grains occurred with an applied DC field from 0 to −1.0 kOe that is a lower negative field than that at room temperature. The applied DC field that caused the simultaneous magnetization reversal in several grains at 150 °C was from +1.5 kOe to 0 kOe (Fig. 4(c)). These data show that magnetization reversal is more likely to occur at elevated temperatures and that the negative magnetic field that causes saturation decreases with increasing temperature.

Note that the extent of simultaneous magnetization reversal also increases with temperature. Although the extent of simultaneous magnetization reversal is a few grains at room temperature, reversal involves several grains at 60 °C and 150 °C. The magnetization reversal beyond the grain boundaries was found to easily occur with increasing temperature because the crystal magnetic anisotropy of Nd–Fe–B decreases and the hard magnetic properties deteriorate. Furthermore, one of the reasons for the increase in the extent of simultaneous magnetization reversal is the decrease in the pinning force of domain wall motion at the grain boundaries at elevated temperatures. The results are consistent with recent work about the influence of the decrease in anisotropy at grain boundaries on the coercivity, as published by Hrkac *et al.*[7,8] Therefore, maintaining a high pinning force at grain boundaries at elevated temperatures is important to realize heat-resistant sintered Nd–Fe–B magnets.

IV. CONCLUSION

In the present study, magnetization reversal and its propagation in sintered Nd–Fe–B magnets at elevated temperatures up to 150 °C were clearly observed using a Kerr microscope, image processing, and photo editing. We found that simultaneous magnetization reversal in several grains along the easy axis direction occurred at elevated temperatures, and the extent of simultaneous magnetization reversal increases with temperature. This indicates that reduction in the coercivity of Nd–Fe–B sintered magnets at elevated temperatures is attributable to a decrease in anisotropy and insufficient pinning of domain walls at grain boundaries. In our future work, it will be necessary to investigate the relationship between simultaneous magnetization reversal and the microstructure of Nd–Fe–B sintered magnets.

[1]S. Hirosawa, T. Nishiuchi, N. Nozawa, T. Ohkubo, K. Hono, H. Sepehri-Amin, M. Takezawa, J. Yamasaki, S. Yamanuro, T. Tanaka, M. Okano, and K. Sumiyama, in *Proceedings of the 21st Workshop on Rare-Earth Permanent Magnets and their Applications*, Bled, Slovania, 2010, p. 187.
[2]S. Sugimoto, J. Jpn. Soc. Powder Powder Metall. **57**, 395 (2010).
[3]D. Li and K. J. Strnat, J. Appl. Phys. **57**, 4143 (1985).
[4]M. Takezawa, T. Shimada, S. Kondo, S. Mimura, Y. Morimoto, T. Hidaka, and J. Yamasaki, J. Appl. Phys. **101**, 09K106 (2007).
[5]M. Takezawa, Y. Kimura, Y. Morimoto, and J. Yamasaki, IEEE Trans. Magn. **49**, 3262 (2013).
[6]M. Takezawa, Y. Ichihara, Y. Morimoto, and J. Yamasaki, IEEE Trans. Magn. **45**, 4439 (2009).
[7]G. Hrkac, T. G. Woodcock, C. Freeman, A. Goncharov, J. Dean, T. Schrefl, and O. Gutfleisch, Appl. Phys. Lett. **97**, 232511 (2010).
[8]T. G. Woodcock, Y. Zhang, G. Hrkac, G. Ciuta, N. M. Dempsey, T. Shrefl, O. Gutfleisch, and D. Givord, Scr. Mater. **67**, 536 (2012).